

Modulation of Fronto-Cortical Activity by Modafinil: A Functional Imaging and Fos Study in the Rat

Alessandro Gozzi*¹, Valeria Colavito², Paul F Seke Etet², Dino Montanari³, Silvia Fiorini⁴, Stefano Tambalo⁴, Angelo Bifone¹, Gigliola Grassi Zucconi² and Marina Bentivoglio²

¹Center for Nanotechnology Innovation @NEST, Istituto Italiano di Tecnologia, Pisa, Italy; ²Department of Neurological Sciences (DSNNMM), University of Verona, Verona, Italy; ³GlaxoSmithKline Medicines Research Centre, Verona, Italy; ⁴Department of Computer Sciences, University of Verona, Verona, Italy

Modafinil (MOD) is a wake-promoting drug with pro-cognitive properties. Despite its increasing use, the neuronal substrates of MOD action remain elusive. In particular, animal studies have highlighted a putative role of diencephalic areas as primary neuronal substrate of MOD action, with inconsistent evidence of recruitment of fronto-cortical areas despite the established pro-cognitive effects of the drug. Moreover, most animal studies have employed doses of MOD of limited clinical relevance. We used pharmacological magnetic resonance imaging (phMRI) in the anesthetized rat to map the circuitry activated by a MOD dose producing clinically relevant plasma exposure, as here ascertained by pharmacokinetic measurements. We observed prominent and sustained activation of the prefrontal and cingulate cortex, together with weaker but significant activation of the somatosensory cortex, medial thalamic domains, hippocampus, ventral striatum and dorsal raphe. Correlation analysis of phMRI data highlighted enhanced connectivity within a neural network including dopamine projections from the ventral tegmental area to the nucleus accumbens. The pro-arousing effect of MOD was assessed using electroencephalographic recording under anesthetic conditions comparable to those used for phMRI, together with the corresponding Fos immunoreactivity distribution. MOD produced electroencephalogram desynchronization, resulting in reduced delta and increased theta frequency bands, and a pattern of Fos induction largely consistent with the phMRI study. Altogether, these findings show that clinically relevant MOD doses can robustly activate fronto-cortical areas involved in higher cognitive functions and a network of pro-arousing areas, which provide a plausible substrate for the wake-promoting and pro-cognitive effects of the drug. *Neuropsychopharmacology* (2012) **37**, 822–837; doi:10.1038/npp.2011.260; published online 2 November 2011

Keywords: pharmacological MRI; cognition; EEG; fMRI; fronto-cortical areas; psychostimulant drugs

INTRODUCTION

The drug modafinil (MOD) is a wake-promoting agent clinically used for the treatment of sleep disorders including narcolepsy, sleep apnea and shift-work sleep disorders. In addition to enhancing wakefulness, many recent studies support an effect of the drug as cognitive enhancer. MOD was shown to robustly enhance alertness and attenuate impairments in tests of mental performance in sleep-deprived volunteers, and similarly, albeit weaker, cognitive improvements have been observed in non sleep-deprived subjects (Pigeau *et al*, 1995; Wesensten *et al*, 2002). These results have prompted an increased off-label use of MOD for the treatment of cognitive dysfunction in some

psychiatric disorders (ie, schizophrenia and attention-deficit/hyperactivity disorder). Encouraging results have been reported from initial single-dose studies in these conditions (Baranski *et al*, 2004; Turner *et al*, 2003; Repantis *et al*, 2010), but repeated dose trials have hitherto failed to demonstrate significant improvements (Freudenreich *et al*, 2009; Pierre *et al*, 2007). Importantly, non-medical use of MOD by healthy individuals has increased in recent years with the expectation of cognitive performance improvements (Repantis *et al*, 2010).

Despite the increasing interest into the properties of MOD, the specific brain substrates underlying the effects of the drug remain to be fully elucidated (Lynch *et al*, 2011). This void is especially relevant for neuropsychiatry research, because clarification of the circuits mediating MOD action may yield leads for the development of effective cognitive-enhancing therapeutics.

Animal research on the central substrates of MOD action has been based on a variety of MOD doses and routes of administration that have hitherto produced inconsistent results. Early studies based on Fos as marker of neuronal

*Correspondence: Dr A Gozzi, Center for Nanotechnology Innovation @NEST, Istituto Italiano di Tecnologia, Piazza San Silvestro 12, 56127 Pisa, Italy, Tel: +39 050 509032, Fax: +39 050 509417, E-mail: alessandro.gozzi@iit.it
Received 10 March 2011; revised 10 September 2011; accepted 19 September 2011

activation induced by MOD administration in the cat (5 mg/kg, p.o.) and rat (300 mg/kg, i.p.) have pointed to the anterior and paraventricular hypothalamic areas as key substrates of MOD action (Lin *et al*, 1996; Engber *et al*, 1998). The effect, however, was not reproduced in subsequent studies in the rat (75 and 150 mg/kg, i.p.; Scammell *et al*, 2000) and mouse (100 mg/kg, i.p.; Willie *et al*, 2005), in which a dose-dependent contribution of cortical and striatal areas was instead observed. On the other hand, deoxyglucose metabolic mapping in the rat after MOD administration (150 and 300 mg/kg, i.p.) has demonstrated increased activity of the hippocampus, thalamus and amygdala, but no involvement of cortical, striatal or hypothalamic areas (Engber *et al*, 1998). Importantly, both the neurochemical effects of MOD and regional Fos induction (Fiocchi *et al*, 2009; Scammell *et al*, 2000) have been shown to be dependent on the dose of MOD used. Since a very wide range of MOD doses (5–600 mg/kg) has been employed in animal studies, their clinical relevance remains to be determined.

Pharmacological and neurochemical studies have revealed an effect of MOD on multiple neurotransmitter systems. Catecholamines appear to have a predominant role in mediating MOD effects on waking and activity, an action that underlies downstream contributions from other neurotransmitters such as histamine, serotonin and orexin (reviewed by Minzenberg and Carter, 2007). Furthermore, MOD decreases GABA in some regions, possibly as a consequence of its ability to increase central glutamate levels (Kumar, 2008). However, the extent to which such complex cascade affects specific neuronal targets remains to be defined.

Spatially resolved imaging techniques such as pharmacological magnetic resonance imaging (phMRI) permit to non-invasively map the neural circuits engaged by psychoactive agents (Honey and Bullmore, 2004). Recent human neuroimaging studies have provided some initial insights into the site of action of MOD. Increased perfusion in the thalamus, dorsal pons, fronto-cortical areas and hippocampus was observed in healthy volunteers receiving MOD at a dose of 400 mg/kg (Joo *et al*, 2008). Likewise, imaging studies of cognitive function have indicated an improvement in information processing within the prefrontal cortex after MOD use in normal volunteers (Saletu *et al*, 2007), as well as in narcoleptic and schizophrenic patients (Hunter *et al*, 2006; Spence *et al*, 2005). Thus, the limited human neuroimaging evidence available highlights a major contribution of fronto-cortical systems to the pro-cognitive and wake-promoting properties of MOD.

Here, we used phMRI to spatially resolve the neural circuitry modulated by MOD in the rat testing a MOD dose that produces clinically relevant blood exposure. The protocol we employed relies on the measurement of cerebral blood volume (CBV), an established marker of brain metabolism (Gaisler-Salomon *et al*, 2009; Small *et al*, 2004), under controlled anesthetic conditions. Recent studies with the same protocol have highlighted an encouraging correspondence with functional readouts in freely moving animals, and analogous human fMRI results (reviewed by Bifone and Gozzi, 2010). Correlation analysis of phMRI time series was also performed to identify a modulatory effect of MOD on neural functional connectivity

(Bifone *et al*, 2010). Finally, to corroborate the functional significance of the imaging results, we assessed the arousing effect of MOD under the anesthetic conditions of the study using electroencephalogram (EEG) recordings, and analyzed in the same subjects Fos immunoreactivity distribution.

MATERIALS AND METHODS

All animal procedures were performed under approval of the University of Verona (Interdepartmental Center for Animal Care and Use Committee), GlaxoSmithKline and Italian Ministry of Health, following the National Institute of Health Guide for the Use and Care of Laboratory Animals, and in accordance with the European Communities Council Directives (86/609/EEC).

Animals

Sprague-Dawley male rats (Harlan, S Pietro al Natisone, Italy) weighing 250–350 g were used. The animals were housed three per cage for at least 10 days before the experiments, with free access to food and water, under a 12 h:12 h light-dark cycle (lights on at 0700 h) and constant room temperature. All the experiments were conducted during the light phase, between 1000 and 1400 h, notably corresponding to the peak of the resting phase of the animal rest-activity 24 h cycle.

Drug Administration

MOD (Sigma-Aldrich, Milan, Italy) was suspended in saline containing 5% dimethyl-sulfoxide (DMSO). The drug was initially dissolved in DMSO and then brought to the desired volume using saline. Drug suspensions were always prepared immediately before administration to avoid compound precipitation, and a dose of 10 mg/kg was used for intravenous (i.v.) administration of the drug. Control subjects received 3 ml/kg of vehicle (5% DMSO in saline).

Plasma Exposure of MOD

Pharmacokinetic parameters for MOD upon i.v. administration have been previously reported (Yu *et al*, 2000). Based on the published data, we estimated that a dose of 10 mg/kg would ensure a clinically relevant plasma exposure. To confirm this, we measured the plasma concentration produced 1 h after i.v. administration of MOD 10 mg/kg in a satellite group of animals ($N=3$), using the same formulation and anesthetic conditions employed for the imaging and EEG recording studies.

Blood sampling and pharmacokinetic analysis were performed as previously described (Ferrari *et al*, 2010). Briefly, plasma samples were obtained, and N,N-dimethyl-formamide (10 μ l/100 μ l plasma) was added to each tube. Samples were prepared for analysis by the addition of two volumes of cold acetonitrile containing an internal standard. Upon centrifugation, the supernatant was removed, the amount of MOD analyzed by liquid chromatography/tandem mass spectrometry. The concentration of MOD in the samples was quantified against a rat plasma standard curve made via serial dilution in a concentration ranging

from 5 to 40 000 ng/ml. Pharmacokinetic parameters were estimated for each rat by non-compartmental analysis of the plasma concentration *vs* time data using the WinNonlin software (Professional Version 4.0.1, Pharsight Corporation, Palo Alto, CA, 1997).

phMRI

Animal preparation/monitoring and MRI acquisition parameters have been described in detail in previous publications (Gozzi *et al.*, 2008b, 2010), and are here briefly presented. The rats were anesthetized with halothane, tracheotomized and artificially ventilated under neuromuscular blockade. After surgery the halothane level was set to 0.8%. The ventilation parameters were adjusted to maintain normocapnic arterial CO₂ levels (Pepelko and Dixon, 1975). No statistically significant difference in the pre- and post-acquisition p_aCO₂ values between groups was found (one-way analysis of variance, ANOVA, dof = 14, $F(2,13) = 0.86$; $p = 0.45$). Linear regression analysis did not show a significant correlation between the amplitude of the relative CBV (rCBV) in response to MOD in the prefrontal cortex (rebinned over a 4–20-min post injection time window) and p_aCO₂ levels, when these were expressed as individual measurements, or pre- and post-acquisition difference ($p > 0.31$, all tests; data not shown). P_aO₂ levels were >90 mmHg in all subjects, corresponding to >98% hemoglobin saturation.

MRI data were acquired using a Bruker Avance 4.7 Tesla system. A 72-mm birdcage resonator was used for radio-frequency (RF) transmit and a Bruker quadrature 'Rat Brain' coil, placed dorsally on the skull of the animal, was used for RF receive. The MR acquisition comprised T₂-weighted anatomical images using a fast spin-echo sequence (TR = 5000 ms, TE_{eff} = 76 ms, RARE factor = 8, FOV = 40 mm, 256 × 256 matrix, 20 contiguous 1 mm slices) followed by a time series acquisition with the same spatial coverage and similar parameters (TR = 2700 ms, TE_{eff} = 110 ms, RARE factor = 32), but with a lower in-plane spatial resolution (128 × 128), with a resulting time resolution of 27 s per brain volume. Following five reference images, superparamagnetic iron oxide particles (Endorem, Guerbet, Genoa, Italy; 2.67 ml/kg) were injected i.v. to enable acquisition of images reflecting alterations in microvascular CBV (Mandeville *et al.*, 1998; Boxerman *et al.*, 1995). After 25 min, each subject received an i.v. challenge with vehicle ($N = 7$) or MOD (10 mg/kg; $N = 9$). Total MRI time series acquisition time was 57 min (128 repetitions).

phMRI Data Analysis

CBV time series images were analyzed within the framework of the general linear model (GLM) as previously described (Worsley *et al.*, 1992; Gozzi *et al.*, 2008c). Signal intensity changes were converted into fractional CBV using a constrained exponential model of the gradual elimination of the contrast agent from the blood (Schwarz *et al.*, 2003). Individual subjects were spatially normalized to a stereotaxic rat brain MRI template set as previously described (Schwarz *et al.*, 2006a). rCBV time series were calculated covering a 7.2-min (16 time points) pre-challenge baseline and 25.0-min (56 time points) post-challenge window.

Image-based time series analysis was carried out using the FMRI Expert Analysis Tool Version 5.63, part of the FSL software (Smith *et al.*, 2004) with 0.8 mm spatial smoothing and a model function capturing the temporal profile of the signal change induced by the MOD challenge (Schwarz *et al.*, 2006a,b). The model function was identified by wavelet cluster analysis (WCA) as previously described (Schwarz *et al.*, 2006b). The WCA regressor chosen captured very well the sustained positive rCBV changes produced by the drug challenge as seen with volume of interest (VOI)-based analysis (Supplementary Figure S1). Higher level group comparisons were carried out using the FSL software with multi-level Bayesian (FLAME) inference; Z-statistics images were thresholded using clusters determined by $Z > 2.3$ and a corrected cluster significance of $p = 0.01$. Cluster correction is a familywise-error correction approach implemented in FSL that introduces a multiplicity correction with respect to the size of activated clusters. A detailed description of the method has been reported elsewhere (Worsley *et al.*, 1992; Friston *et al.*, 1994). A GLM analysis performed with a boxcar function (off (1 : 15) and on (16–56)) reproduced the activation map obtained with the WCA regressor (data not shown).

phMRI time courses for MOD or vehicle in anatomical VOIs were extracted from unsmoothed time series using a 3D digital reconstruction of a rat brain atlas (Paxinos and Watson, 2005) co-registered with the MRI template (Schwarz *et al.*, 2006a). For each VOI, the mean rCBV over a 10-min time window (13–23 min post injection) covering the plateaued response produced by MOD was used as summary statistics. A similar approach has been recently applied to assess the functional response produced by i.v. injection of the psychostimulant agent D-amphetamine under identical experimental conditions (Gozzi *et al.*, 2011). For this reason, averaged D-amphetamine-induced response has also been here used to illustrate the comparison with MOD.

Intersubject functional connectivity analysis with respect to reference brain regions was performed as previously described (Schwarz *et al.*, 2007a,b, 2009). Briefly, maps of response amplitudes correlating across subjects with the responses in a reference brain region were calculated within the GLM framework at the group level using FSL/FLAME as mentioned above. A number of reference VOIs was examined: ventral tegmental area, prefrontal cortex, cingulate cortex, somatosensory cortex, caudate-putamen, nucleus accumbens, thalamus, ventral hippocampus and dorsal raphe. Z-statistics images were calculated via contrasts capturing positive and negative correlations with the reference response, and thresholded at $Z > 2.3$ and a corrected cluster significance threshold of $p = 0.05/N$, where N is the number of subjects per group (MOD = 9, vehicle = 7). Linear regression plots of correlated rCBV responses were calculated by plotting mean rCBV response to MOD across individual subjects, the latter being expressed as mean response over a 20-min (4–24 min post injection) time window.

The nomenclature was based on the Paxinos and Watson (2005) atlas of the rat brain, except for the prefrontal cortex (not indicated as such in this atlas). In agreement with anatomical and behavioral studies in the rat (see Uylings *et al.*, 2003 for a review), we here indicate as prefrontal

cortex the prelimbic and infralimbic cortex as delineated by Paxinos and Watson (2005), considering separately the anterior cingulate cortex.

EEG and Fos Investigation

Rats were placed into a knockdown anesthesia box chamber while carefully minimizing the potential interference of external stimuli and reducing the handling time to <2 min per subject. Anesthesia was induced with 3% halothane. The animals were then randomly assigned to MOD ($N=6$) or vehicle (control) ($N=4$) groups, and equipped with a cannula inserted into a tail vein and a transcutaneous carbon dioxide tension (tcPCO₂) monitor (Ramos-Cabrer *et al*, 2005).

Accessory experiments performed in our laboratory have shown a strong linear relationship between transcutaneous and arterial p_aCO₂ measurements ($N=110$, $R^2=0.98$), so that transcutaneous values present a stable $\sim +10$ mmHg offset with respect to the corresponding arterial measurements (data not shown).

During the same procedure, rats were implanted with electrodes for acute EEG recording. To this purpose, craniometric data for adult Sprague-Dawley rat were extrapolated on the scalp of the intact animal by assessing distances rostrally to the supraoccipital bone (recognizable to the touch) corresponding to the parietal and frontal bones (12 and 21 mm, respectively), and on the right side of the midline (1–2 mm). At these coordinates, two needle electrodes (4 cm in length and 0.7 mm in diameter) were inserted subcutaneously on the skull and fixed. A third electrode was placed in the orbital region as reference electrode. This positioning of electrodes has been widely validated for EEG recordings comparable to those obtained by chronic implants (Vanderwolf, 1992; Weiergrasber *et al*, 2005; Birbaumer *et al*, 2008). After electrode implantation, the level of halothane was adjusted to achieve a stable (at least 30 min) uninterrupted presence of slow-wave delta (0.3–4 Hz) activity (Antunes *et al*, 2003). This procedure has been previously applied to the characterization of the arousing effect of amphetamine under halothane anesthesia (Berridge and Morris, 2000). Stable EEG traces were obtained with nominal halothane levels between 1.2 and 1.5%. These halothane concentrations have been shown not to suppress Fos expression in the rat brain and spinal cord under different stimulation paradigms (Novikova *et al*, 2004; Sun *et al*, 1996).

EEG Recording and Analysis

Rats underwent EEG monitoring for 40–45 min under basal conditions and for 100 min following MOD administration. EEG activity was monitored using the Twin EEG Recording System connected with a Comet AS-40 amplifier (Grass Telefactor, West Warwick, RI). The EEG signals were bandpass-filtered (0.1 Hz highpass and 70 Hz lowpass cutoff), digitized and stored at a sampling rate of 200 Hz using the TWin software (Grass Telefactor). EEG signals before and after vehicle or MOD administration were analyzed and compared. A pre-injection segment was defined as the 25-min epoch before MOD or vehicle injection. The post-administration segment was defined as

a 25-min epoch starting 5 min after drug injection. The 5-min interval was introduced to exclude non-specific effects related to the administration procedure. For each subject, individual EEG epochs were Fourier transformed and subjected to power spectral analysis (PSA). The resulting data were normalized by expressing the power of each frequency bin as a proportion of the total power (relative power) in the 0.3–20-Hz band. The mean power spectrum for each group was calculated in the 0.3–4-Hz (delta) and 4.25–8-Hz (theta) frequency bands. Between-group statistical analysis was performed using one-way ANOVA. Transcutaneous p_aCO₂ levels were between 55 and 65 mmHg in all animals, corresponding to arterial values of ~ 45 –55 mmHg, in line with previous EEG assessment under similar anesthetic conditions in spontaneously breathing animals (Hudetz, 2002; Steriade *et al*, 1994). At the end of the experimental session, the animals were killed by halothane overdose and perfused transcardially as indicated below.

Fos Immunocytochemistry

After an interval of 1 h and 40 min from MOD or vehicle administration, rats were perfused transcardially under halothane anesthesia with 50 ml of 0.1 M phosphate-buffered saline, pH 7.3 (PBS), followed by 300 ml of 4% paraformaldehyde in PBS. The brains were removed, briefly post-fixed, soaked in 20% sucrose until they sank, and then coronally sectioned at 40 μ m on a freezing microtome. Two adjacent series of sections were collected at 200 μ m intervals. One series of sections was processed free floating for Fos immunocytochemistry, and the adjacent series was mounted on gelatinized slides and stained with 0.1% cresyl violet for cytoarchitectonic reference. For Fos immunocytochemistry, the sections were first soaked in 0.3% Triton X-100 (Sigma-Aldrich, Milan, Italy) in PBS (3 \times 5 min rinses) and processed at room temperature unless otherwise indicated. After washing in PBS, the sections were pre-incubated for 1 h in a solution of 0.3% Triton X-100 (Sigma-Aldrich) and 5% normal horse serum (NHS, Vector Laboratories, Burlingame, CA) in PBS. Next, the sections were incubated at 4°C for 36–48 h with goat anti-c-Fos polyclonal antibodies (Santa Cruz Biotechnology, Santa Cruz, CA), diluted 1:4000 in 1% NHS and 0.2% Triton X-100 in PBS. The sections were then incubated for 1 h in biotinylated horse anti-goat antibodies (Vector Laboratories; 1:200 in 1% NHS in PBS), and processed using the avidin-biotin protocol (Standard Vectastain Elite Kit, Vector Laboratories) for 1 h. The reaction was developed using 3-3'-diaminobenzidine as chromogen and nickel intensification (0.025% diaminobenzidine, 0.03% H₂O₂, 0.05% NiCl₂) to obtain a black reaction product. The sections were then washed, mounted on gelatinized slides and coverslipped with Entellan (Merck, Darmstadt, Germany).

For each animal, the distribution of Fos-immunoreactive cells was examined throughout the brain. Two investigators, blind to the experimental group, performed the analyses using an Olympus microscope. Brain regions were identified according to the Paxinos and Watson (2005) brain atlas. Images were digitized using a digital camera (KY-F58 CCD camera, JVC) connected to the microscope.

Quantification of Fos immunoreactivity was performed in representative brain areas (Supplementary Figure S2). The number of Fos-labeled cells in each area was counted in coronal brain sections using an unbiased approach based on region of interest (ROI) sampling. Areas were analyzed on the basis of previous studies on Fos induction elicited by MOD in the rat (Scammell *et al.*, 2000), as well as on Fos profiling induced by other psychoactive drugs (Sumner *et al.*, 2004), and our own data on Fos induction in the cerebral cortex during EEG-assessed wakefulness (Grassi-Zucconi *et al.*, 1994). On this basis, the following areas were analyzed: prefrontal cortex (defined as indicated above to include the prelimbic and infralimbic portions of the cortex) and cingulate cortex; somatosensory cortex, evaluating separately superficial and deep layers (by placing the frame at the brain surface and white matter border, respectively); dentate gyrus of the ventral hippocampus; septum; medial portion of the caudate-putamen; core and shell divisions of the nucleus accumbens; bed nucleus of the stria terminalis; basal forebrain; anterior hypothalamic area; posterior hypothalamic area, including the perifornical region; centromedial and basolateral nuclei of the amygdala; paraventricular and central medial thalamic nuclei, which are components of thalamic midline and anterior intralaminar nuclei, respectively; dorsal raphe nucleus in the brainstem.

For the quantitative analyses, following delineation of each brain region based on adjacent Nissl-stained sections and on anatomical landmarks, an automated counting procedure based on ROI sampling was applied using the image analysis system ImagePro Plus 4.5 (Media Cybernetics, Silver Spring, MD). The counts were obtained in one focal plane, using a $\times 10$ objective, from frames (0.6×0.5 mm) placed bilaterally within each ROI (Supplementary Figure S2); for large ROIs, multiple frames were used. For each ROI, counts were performed in two adjacent sections and averaged. Parameters such as size, shape and threshold gray were optimized for the detection of Fos-positive cells (notably characterized by nuclear immunostaining) and applied to all sections. Background intensity was kept constant across sections so that the counting unit was a cell in which Fos immunolabeling reached a defined optical density threshold above background. In a pilot study, such procedure showed a close agreement between manual and automated cell counting. The criteria adopted in the automated procedure were optimized to exclude lightly immunostained Fos-positive cells, thus resulting in conservative estimates that minimize the contribution of potential false positives due to background staining. Differences in the number of Fos-labeled cells (mean number/frame) between the MOD and control groups were statistically analyzed using the non-parametric Wilcoxon-Mann-Whitney rank sum test. Statistical significance was set at $p \leq 0.05$.

RESULTS

Plasma Exposure

Under the anesthetic conditions used in the imaging study, i.v. administration of 10 mg/kg of MOD (used in all the experiments) produced a plasma exposure of

$0.67 \pm 0.04 \mu\text{g/ml}$ at 1 h post administration. As MOD has a $t_{1/2}$ of 0.2 h in the rat brain (Yu *et al.*, 2000), the predicted exposure of MOD at the end of the pHMRI time window (30 min post injection) was $3.4 \mu\text{g/ml}$. This value is consistent with the range of plasma exposures ($2\text{--}5 \mu\text{g/ml}$) measured in human subjects following oral dosing of clinically effective doses of the drug (ie, 200 mg/kg, Wong *et al.*, 1999; McClellan and Spencer, 1998).

pHMRI

MOD produced a composite, region-specific pattern of functional activation of telencephalic, diencephalic and brainstem regions (Figure 1). Significant rCBV increases were observed in several structures of the telencephalon, including the ventral hippocampus, septum, caudate-putamen and nucleus accumbens. In the cerebral cortex, the most prominent effects were found in fronto-cortical areas, such as the prefrontal, anterior cingulate and orbital cortex. Foci of activation were also documented in the middle and deep layers of the somatosensory cortex throughout its anteroposterior extent. In the diencephalon, activated areas were detected in thalamic domains including the midline and intralaminar nuclei. In the brainstem, focal activation of the dorsal raphe was evident.

The time course of MOD-induced rCBV increase was region dependent (Figure 2). Subcortical and somatosensory cortical regions showed a rapid increase in rCBV, which reached a plateau within 5 min from MOD administration and remained sustained throughout the 25-min time window monitored. In contrast, fronto-cortical areas exhibited a slow-rise gradual increase in rCBV that reached a plateau ~ 20 min after MOD administration. Consistent with previous studies (Gozzi *et al.*, 2006, 2008b), small and transient (~ 3 min) negative rCBV changes were also observed upon MOD or vehicle administration in all the VOIs, probably as a result of temporary dilution of the intravascular contrast agent. No brain region exhibited sustained negative rCBV changes in the MOD group ($Z > 1.6$ vs vehicle).

The magnitude of the rCBV response to MOD was also strictly region dependent (Figure 3), with the largest response in the prefrontal and cingulate cortex ($\sim 20\%$ rCBV increase), and all the other activated regions showing smaller increases ($\sim 8\text{--}10\%$). It has to be noted, in this respect, that the region specificity does not reflect different vascular capacity of different brain areas. Indeed, under identical experimental conditions the psychostimulant D-amphetamine exhibited a different rCBV activation profile (Gozzi *et al.*, 2011), characterized by widespread and uniform activation of multiple forebrain areas and subcortical nuclei (Figure 3; Supplementary Figures S3 and S4; Supplementary Tables S1 and S2).

Intersubject functional connectivity analysis (Schwarz *et al.*, 2007b) was performed by mapping the MOD responses significantly correlating ($Z > 2.3$) with those in the ventral tegmental area (Figure 4), where dopaminergic cell bodies giving origin to the mesolimbic pathway reside. This analysis delineated a discrete network of brain regions corresponding to dopamine projections to the nucleus accumbens. No such correlation was observed in the vehicle group ($Z > 1.9$).

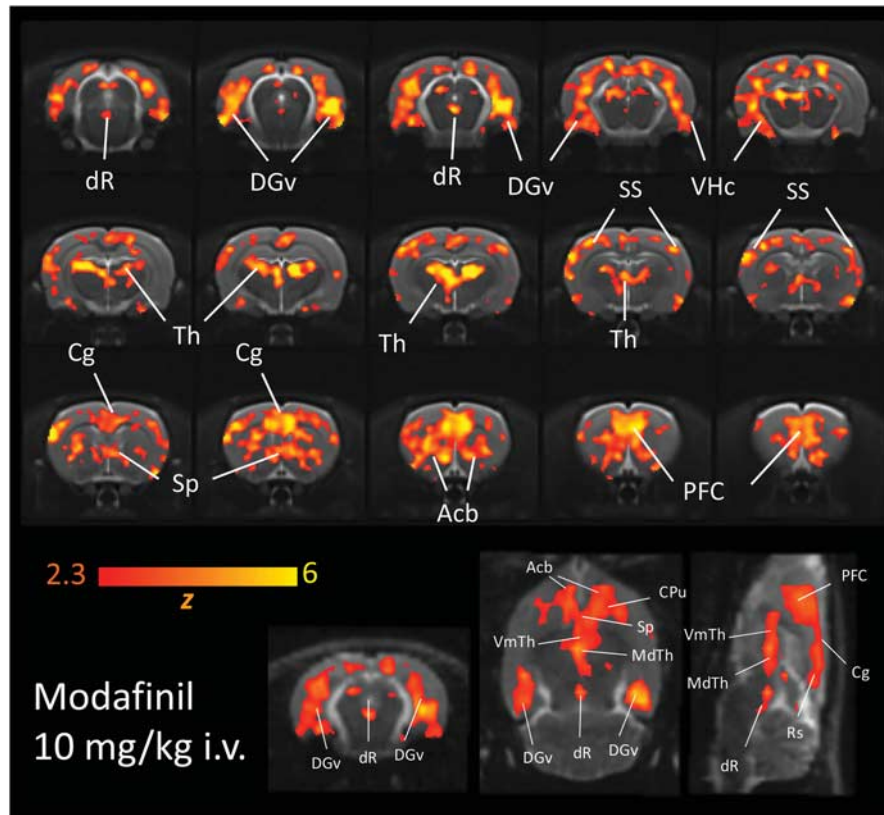


Figure 1 Anatomical distribution of the rat brain regions significantly activated by acute modafinil administration (10 mg/kg i.v.) vs control. The top three rows show contiguous 1 mm-thick coronal slices. The bottom row shows an orthogonal view of the same map including a sagittal and a horizontal slice. Acb, nucleus accumbens; Cg, cingulate cortex; CPu, caudate-putamen; DGv, ventral dentate gyrus; dR, dorsal raphe nucleus; MdTh, midline thalamus; Sp, septum; SS, somatosensory cortex; PFC, prefrontal cortex; Rs, retrosplenial cortex; Th, thalamus; VHc, ventral hippocampus; VmTh, ventromedial thalamus.

MOD and vehicle administration produced transient alterations of mean arterial blood pressure, whose peak magnitude was well within the CBF autoregulation range under the anesthetic conditions used (Supplementary Figure S5). Within this range, abrupt arterial blood pressure changes are homeostatically compensated without resulting in significant microvascular rCBV changes (Gozzi *et al*, 2006, 2007; Zaharchuk *et al*, 1999).

EEG

Under anesthetic conditions similar to those used in the phMRI study, MOD administration produced robust activation of EEG signals within 10–20 min. The PSA analysis highlighted a decreased delta band ($p = 0.007$; one-way ANOVA, dof = 9, $F = 12.89$) and increased theta band ($p = 0.039$; one-way ANOVA, dof = 9, $F = 6.01$) in the MOD group compared with controls (Figure 5). The analysis of PSA of control subjects did not highlight appreciable EEG alterations after vehicle injection.

In the MOD group, EEG tracings revealed two representative patterns of response (Figure 6). The first was characterized by an abrupt shift from slow-wave, large-amplitude activity to high-frequency, low-amplitude activity. The second pattern of response was characterized by bursts of fast activity (lasting 2–3 s), interspersed with longer episodes of slow-wave activity. Both types of response appeared variable in duration (from 30 s to

5 min), and occurred intermittently (at 10–15 min intervals) throughout the period following the drug administration. No noticeable effects on individual EEG tracings were observed in the vehicle group.

Fos Induction

Intergroup quantitative analysis of Fos immunoreactivity highlighted a significant effect of MOD on Fos induction in several brain regions with respect to controls (Figures 7 and 8). In particular, increased numbers of Fos-labeled neurons in the MOD group were observed in fronto-cortical areas such as the prefrontal and cingulate cortex. The effect reached a significant value in the cingulate cortex ($p < 0.02$, Wilcoxon–Mann–Whitney rank sum test, to which all the other p -values of this analysis mentioned below also refer). Significant increases were also found in the septum ($p < 0.02$), caudate-putamen, especially in its medial portion ($p < 0.02$), as well as in the nucleus accumbens ($p < 0.05$ in the shell region). It is noteworthy that all these regions were also found to be significantly activated by MOD in the phMRI study. Furthermore, MOD-induced increases in Fos-labeled neurons were observed in the ventral hippocampus, although only with a trend toward a significant difference vs controls ($p = 0.06$). A similar trend ($p = 0.07$) was also found for MOD-elicited Fos induction in the basal forebrain. At diencephalic level, a significant increase ($p < 0.02$) of MOD-elicited Fos immunoreactivity was

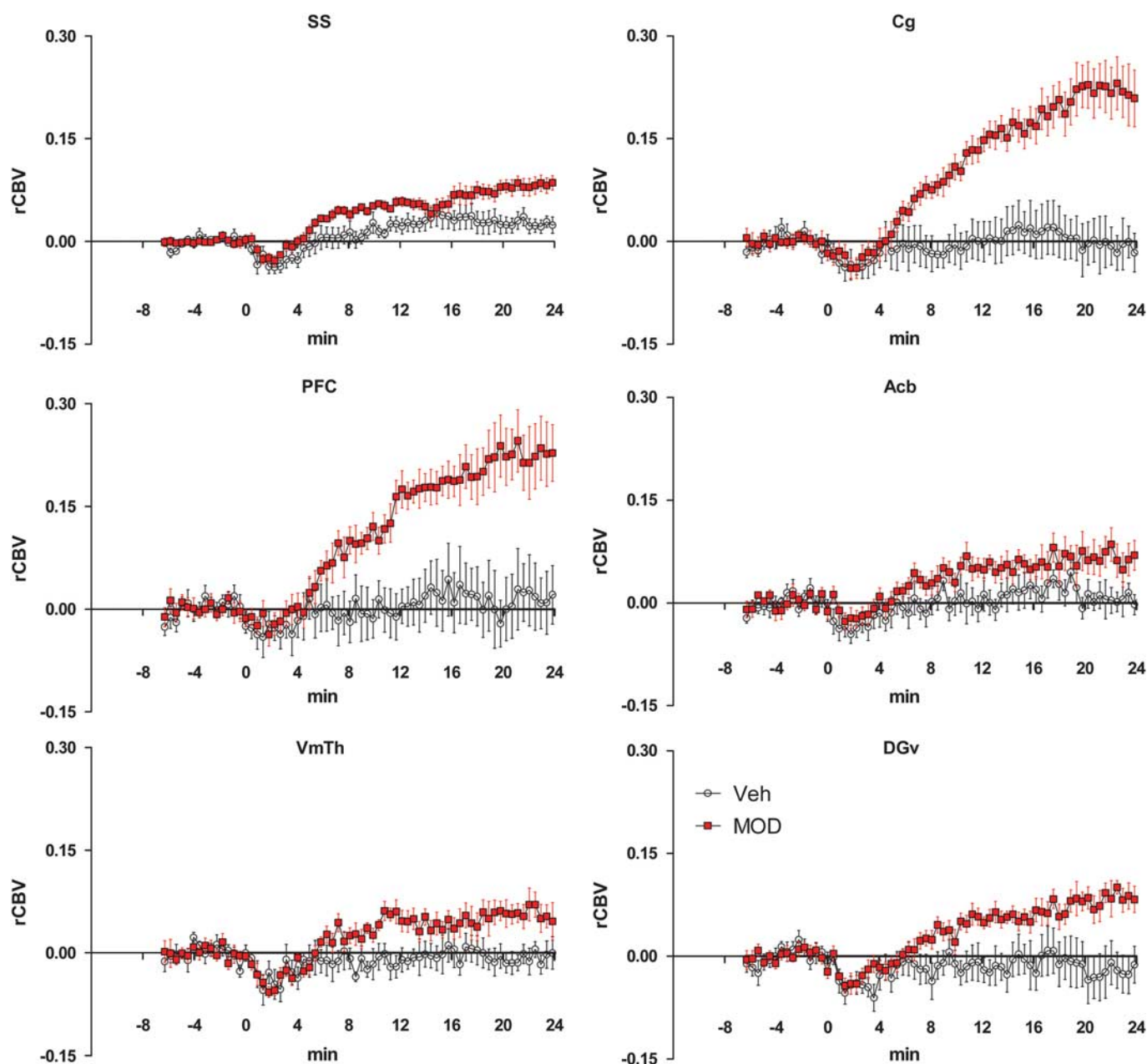


Figure 2 Temporal profile of modafinil-induced relative cerebral blood volume (rCBV) response in representative anatomical volumes of interest. Data are plotted as mean \pm SEM within each group. Acb, nucleus accumbens; Cg, cingulate cortex; DGv, ventral dentate gyrus; PFC, prefrontal cortex; SS, somatosensory cortex; VmTh, ventromedial thalamus.

observed in the anterior intralaminar thalamic nuclei (central medial nucleus), which was also significantly activated in the phMRI study. High Fos induction was also observed in the thalamic paraventricular nucleus located at the midline, and this occurred in both MOD-treated and control groups, as also noted for the anterior and posterior hypothalamic areas, and for the basolateral and especially the central nuclei of the amygdala (for which no activation was detected with phMRI). Likewise, no significant inter-group difference was observed in the dorsal raphe nucleus, which had instead shown activation in the imaging study. No brain areas showed an obvious decrease in Fos immunoreactivity following MOD administration.

Altogether the Fos induction part of the study supported at the cellular level the findings obtained with phMRI, though with some differences which, as discussed below, are in all likelihood due to the different methodological approaches and readout systems.

DISCUSSION

Despite an increasing non-medical and off-label use of MOD, and >20 years of research into the psycho-pharmacological properties of this drug, the neural substrates of its action in the brain remain elusive. In the present study, we

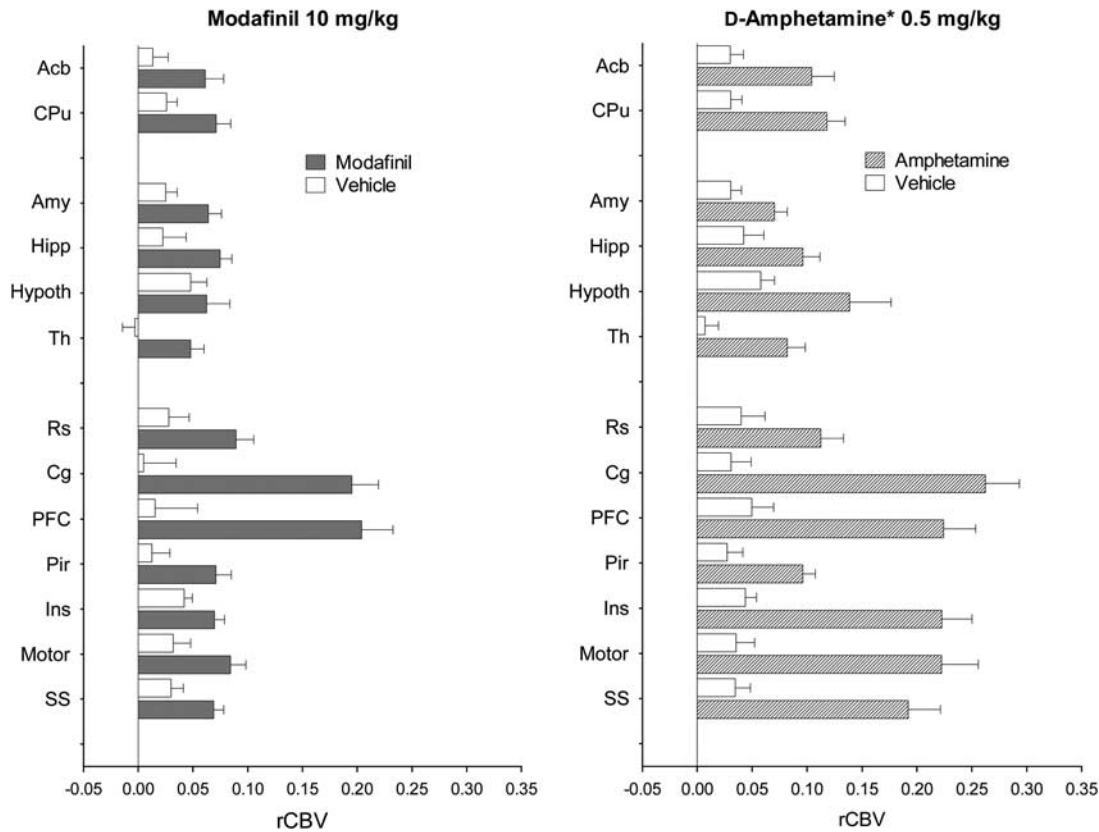


Figure 3 Mean relative cerebral blood volume (rCBV) response in three main groups of representative 3D anatomical volumes of interest: dopamine innervation target areas; medial temporal and diencephalic regions; neocortex and cingulate cortex. Left: modafinil (present study); right: amphetamine (adapted from Gozzi et al, 2011, with permission). Acb, nucleus accumbens; Amy, amygdala; Cg, cingulate cortex; CPu, caudate-putamen; DGv, ventral dentate gyrus; dR, dorsal raphe nucleus; Hipp, hippocampus; Hypoth, hypothalamus; Ins, insular cortex; Motor, motor cortex; PFC, prefrontal cortex; Pir, piriform cortex; Rs, retrosplenial cortex; Sp, septum; SS, somatosensory cortex; Th, thalamus.

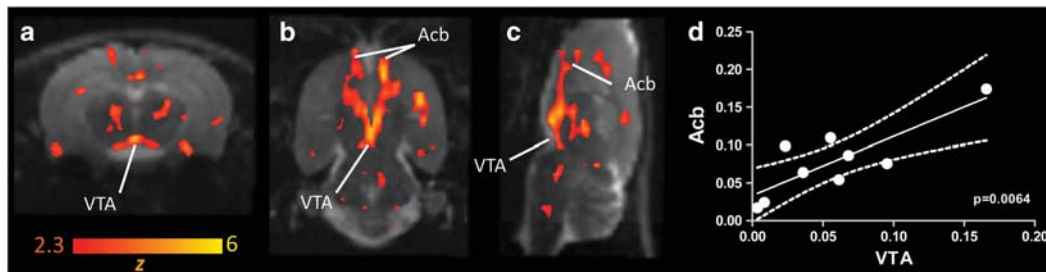


Figure 4 Orthogonal view (a, coronal; b, horizontal; c, sagittal) of the brain regions showing intersubject modafinil responses that correlate with those to the ventral tegmental area (VTA). (d) Correlation (linear regression) between mean relative cerebral blood volume (rCBV) response to modafinil in the nucleus accumbens (Acb) and VTA. *P*-value was calculated using a Student's *t* test on the regression coefficients.

used non-invasive functional imaging to investigate the neuronal circuitry activated by MOD at a dose that produces clinically relevant plasma exposure in the rat. Our data show that MOD can stimulate fronto-cortical areas involved in higher cognitive function, as well as a network of pro-arousing areas, comprising thalamocortical, corticothalamic and dopamine-innervated cell groups. Moreover, MOD treatment was here found to be associated with enhanced connectivity between the dopaminergic ventral tegmental area and its target represented by the nucleus accumbens. Importantly, EEG recordings have here documented a pro-arousing effect of MOD under the anesthetic conditions employed in the pHMRI study, and Fos

immunoreactivity induction has provided an independent confirmation of the functional effect of MOD in several of the regions identified in the imaging study. Overall, the coordinated network of brain structures identified in the present investigation represents a plausible substrate for the wake-promoting and pro-cognitive effects of MOD in the rat.

Functional Response to MOD

The pattern of MOD-elicited activation presents several features relevant to the functional interpretation of the pharmacological effects of the drug. First, the robust

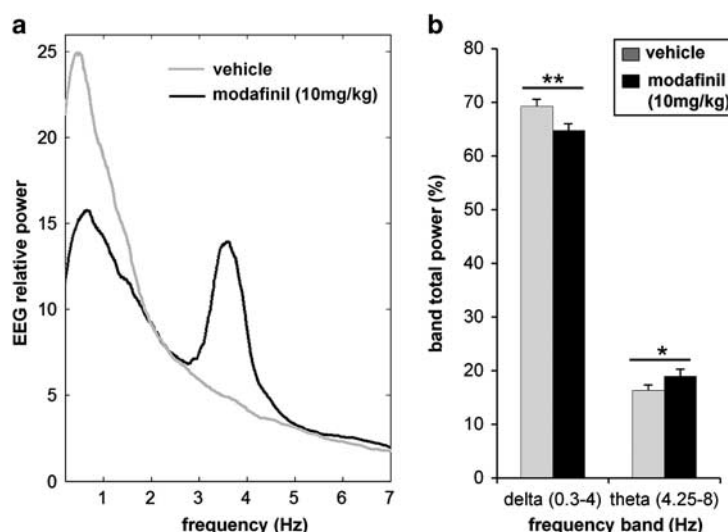


Figure 5 Effect of modafinil on the electroencephalogram (EEG) power spectra of halothane-anesthetized rats over a 25-min post administration time window. (a) Modafinil-treated animals exhibit reduced response in the delta band (0.3–4 Hz) and increased response in the theta band (4.25–8 Hz). (b) Quantification of the effect of modafinil on the EEG power in the delta and theta frequency bands. Data are mean \pm SEM. * $p < 0.05$, ** $p < 0.01$, one-way ANOVA; $N = 4$ vehicle, $N = 6$ MOD.

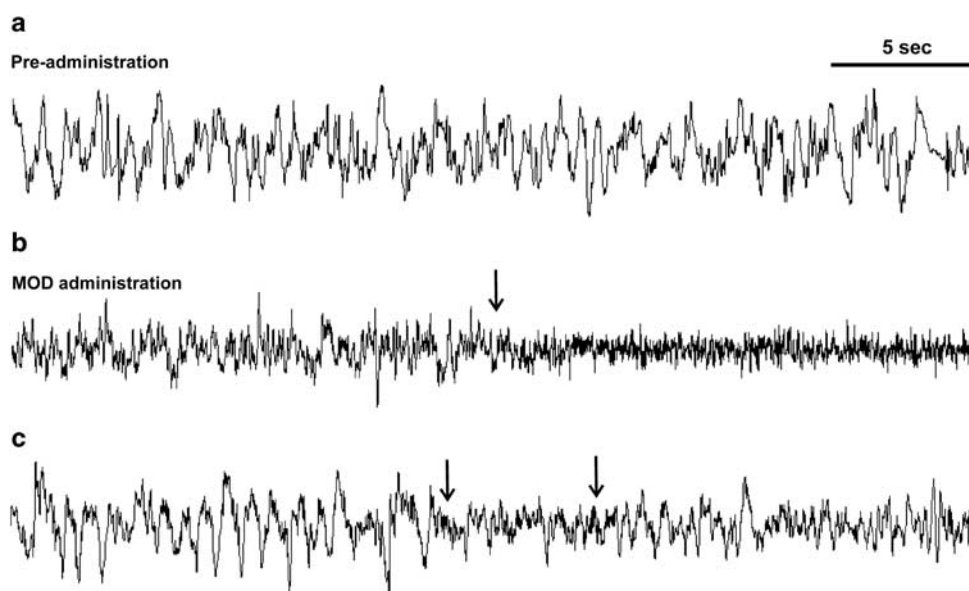


Figure 6 Effect of modafinil (MOD) administration on individual electroencephalogram (EEG) activity traces. (a) Representative 30 s segment of EEG recording sampled immediately before MOD administration. (b, c) Examples of desynchronization observed after MOD administration. In (b), MOD evoked a sudden change (arrow) from slow-wave, large-amplitude activity to high-frequency, low-amplitude activity. In (c), the response is characterized by bursts of low-voltage fast activity intermingled with dominant slow-wave activity (arrows).

activation of fronto-cortical areas is relevant for translational research, as it reconciles preclinical functional mapping data, in which the involvement of fronto-cortical areas has not been consistently observed (Lin *et al*, 1996; Fiocchi *et al*, 2009; Engber *et al*, 1998; Scammell *et al*, 2000), with the increasing evidence in humans of a cortical modulation by the drug in normal (Saletu *et al*, 2007; Joo *et al*, 2008) and impaired states (Hunter *et al*, 2006; Spence *et al*, 2005; Saletu *et al*, 2004; Thomas and Kwong, 2006). The fronto-cortical activation is also consistent with the improved cognitive performance observed in rodent behavioral tasks upon MOD administration at doses similar

to those employed in the present study (Tsanov *et al*, 2007; Beracochea *et al*, 2001, 2003; Dawson *et al*, 2010).

Consistent with the notion that fronto-cortical cognitive tasks are subserved by an extensively interconnected network of regions (reviewed by Mesulam, 1990), additional brain substrates activated by MOD may have a role in the pro-cognitive action of the drug. For example, animal studies demonstrated that integrity of the nucleus accumbens (Floresco *et al*, 2006), mediodorsal thalamic nucleus (Block *et al*, 2007) and posterior parietal cortex (Fox *et al*, 2003) is necessary for specific cognitive processes like perceptual attentional set shifting. This task has been shown

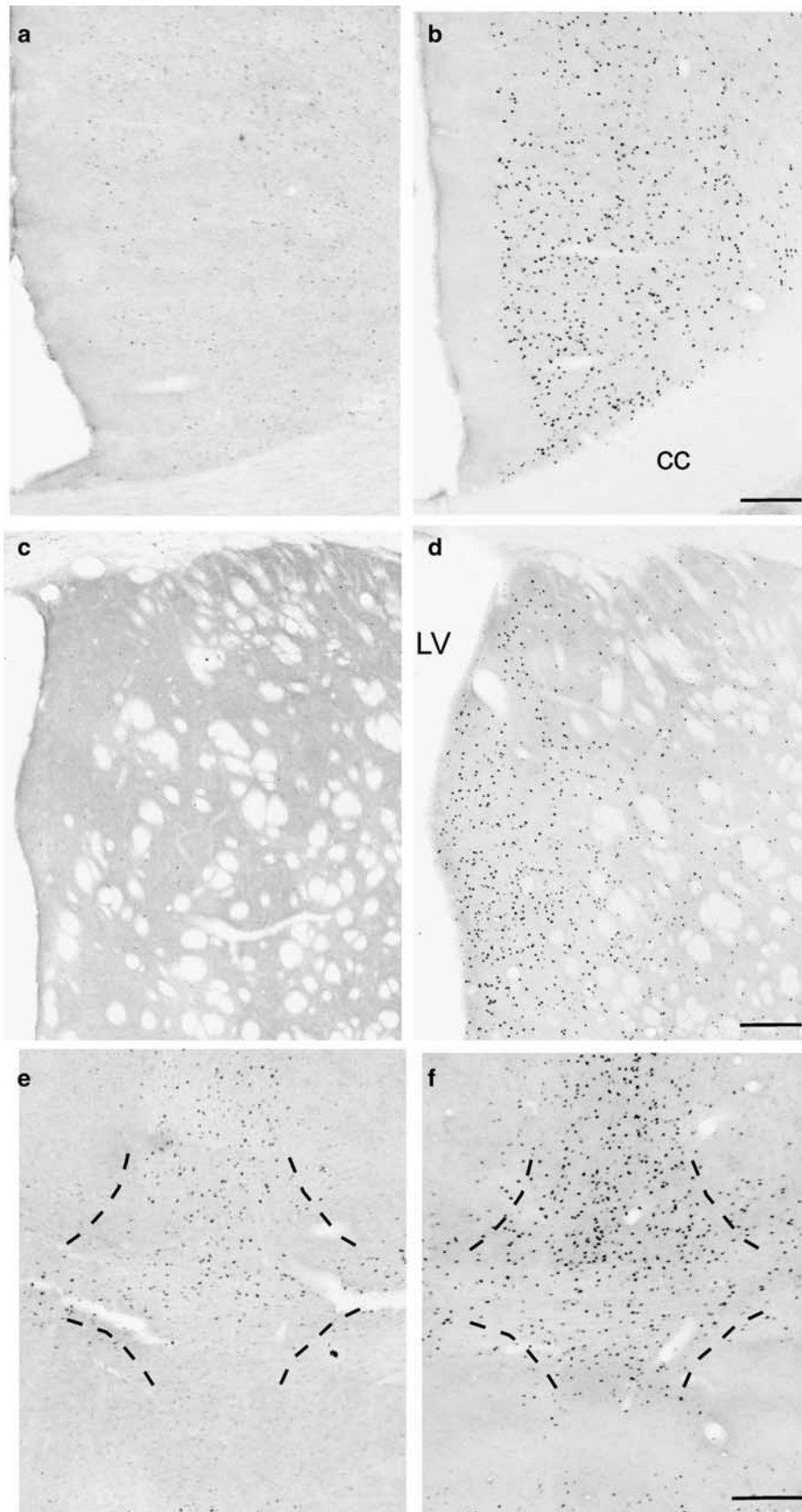


Figure 7 Representative images of Fos immunolabeling after modafinil (MOD) treatment (right column, b, d, f) compared with controls (vehicle, left column, a, c, e) showing that MOD markedly enhanced Fos induction in the cingulate cortex (a, b), medial caudate-putamen (c, d) and thalamic central medial nucleus (delimited by the dotted line in e, f). Scale bars = 200 μ m; cc, corpus callosum; LV, lateral ventricle.

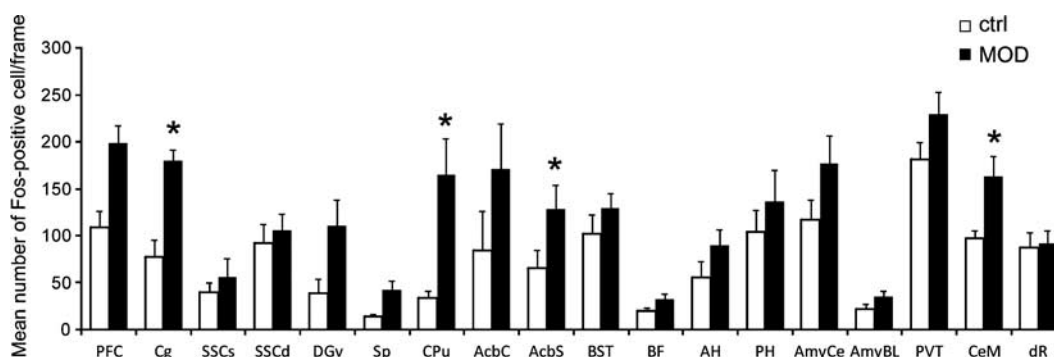


Figure 8 Effect of modafinil (MOD) on the number of Fos-positive cells in regions of interest (ctrl: control animals treated with vehicle). Data are expressed as mean \pm SEM. * $p < 0.05$, Wilcoxon–Mann–Whitney rank sum test. The anatomical distribution of the regions examined is reported in Supplementary Figure S2. AcbC, nucleus accumbens core; AcbS, nucleus accumbens shell; AH, anterior hypothalamus; AmyBL, basolateral nucleus of the amygdala; AmyCe, centromedial nucleus of the amygdala; BST, bed nucleus of the stria terminalis; BF, basal forebrain; CeM, central medial thalamic nuclei; Cg, cingulate cortex; CPu, caudate-putamen; DGv, ventral dentate gyrus; dR, dorsal raphe nucleus; PFC, prefrontal cortex; PH, posterior hypothalamus; PVT, paraventricular thalamic nuclei; Sp, septum; SSCs, somatosensory cortex superficial layers; SSCd, somatosensory cortex deep layers.

to be improved by MOD in animal models of cognitive impairment (Dawson *et al.*, 2010). Similarly, the fronto-septo-hippocampal circuit and its interaction with midline thalamic nuclei are known to have a role in cognitive processing and memory formation (Vertes, 2006; Dalley *et al.*, 2004; Becker *et al.*, 1981; Squire, 1992).

The present imaging findings also highlighted network features that can be related to the wake-promoting effect of MOD. Of these, the activation of thalamic cell groups and of the middle and deep cortical layers, which include thalamocortical fiber innervation and corticothalamic neurons, is of special interest given the known role of thalamocortical systems and corticothalamic control in the regulation of wakefulness and arousal (McCormick and Bal, 1997; Steriade, 1996; Pace-Schott and Hobson, 2002). Among the brainstem nuclei covered by the imaging volume used in the pHMRI study, a clear involvement of the dorsal raphe was evident. This nucleus, which is the main source of serotonergic innervation of the diencephalon and telencephalon, is active during waking and necessary for complete arousal and cortical activation (Espana and Scammell, 2004). This finding is in keeping with *in-vivo* microdialysis data showing increased dialysate serotonin levels in the raphe nucleus upon MOD administration (Ferraro *et al.*, 2002).

Involvement of Dopaminergic Circuits

Mounting preclinical evidence points to a key contribution of dopamine to the wake-promoting properties of MOD. For example, mice lacking dopamine transporters are not sensitive to the wakefulness-promoting effects of MOD (Wisor *et al.*, 2001), as also mice lacking dopamine D₁ and D₂ receptors (Qu *et al.*, 2008). Microdialysis studies have shown that MOD increases extracellular dopamine in the nucleus accumbens and prefrontal cortex (de Saint *et al.*, 2001; Murillo-Rodriguez *et al.*, 2007). In addition, recent positron emission tomography (PET) studies in humans (Volkow *et al.*, 2009) and anesthetized monkeys (Madras *et al.*, 2006) have documented significant occupancy of dopamine transporters in the nucleus accumbens and caudate-putamen upon administration of MOD. Consistently

with these results, we observed focal and sustained activation of the caudate-putamen and nucleus accumbens in pHMRI maps of MOD-treated subjects. Moreover, functional connectivity analysis of pHMRI responses correlating with the ventral tegmental area delineated the longitudinal extension of the mesolimbic dopamine pathway to the nucleus accumbens in the MOD group, but not in controls. Taken together, our findings are consistent with a pivotal contribution of dopamine pathways to the effect of MOD, and suggest that the drug may enhance functional connectivity in the mesolimbic pathway.

The activation of a mediator of reinforcement such as the nucleus accumbens (Salamone and Correa, 2002) is also of interest in the light of the debated abuse potential of MOD (Kruszewski, 2006). The drug was shown to be self-administered in monkeys previously trained to self-administer cocaine (Newman *et al.*, 2010; Gold and Balster, 1996), and may act as a reinforcer under conditions of behavioral demands (Stoops *et al.*, 2005). It should, however, be emphasized that the reinforcing and psychostimulant properties of MOD are weaker than those of classical dopamine-mimetic stimulants, so that the effective abuse liability of MOD at clinical doses remains limited and clinical reports of MOD abuse are rare (Jasinski, 2000; Myrick *et al.*, 2004).

Comparison with Amphetamines

Converging evidence from studies in animal models and humans suggests that the distinctive psychotropic properties of MOD compared with traditional psychostimulants (ie, amphetamines) reflect a unique neurochemical profile (Minzenberg and Carter, 2007). For example, MOD displays significant affinity but low potency at dopamine transporter and norepinephrine transporter leading to moderate elevations in extracellular dopamine and norepinephrine levels (Madras *et al.*, 2006). MOD administration has also been shown to affect other multiple neurotransmitter systems, including GABA, serotonin, glutamate, orexin and histamine, possibly secondary to catecholamine effects (Minzenberg and Carter, 2007; Qu *et al.*, 2008).

Our imaging results allow to compare MOD and amphetamine action under identical experimental conditions. In a recent study (Gozzi *et al.*, 2011), we used the same phMRI protocol to map the effects of a dose of amphetamine that, in keeping with the present data with MOD, was previously shown to elicit a pro-arousing effect in EEG recording in halothane-anesthetized animals (Berridge and Morris, 2000). Unlike MOD, amphetamine produced widespread and robust activation of the forebrain with no sign of cortical layer specificity. Moreover, the effect of amphetamine was robust and quantitatively comparable across cortical regions (Gozzi *et al.*, 2011), and lacked much of the subcortical and fronto-cortical specificity observed with MOD. These findings are consistent with the different pharmacological profile of the two drugs (Minzenberg and Carter, 2007), and suggest that MOD can focally activate brain substrates of arousal and cognition, which, in the case of amphetamine, appear to be recruited as a result of a global psychostimulant effect.

Fos Induction

The present results of Fos induction analysis have documented significant MOD-induced increases in a network of areas including fronto-cortical regions, caudate-putamen, nucleus accumbens and medial thalamic domains, all of which exhibited significant rCBV increases in response to the drug. Given the independent nature of cellular (ie, Fos induction) and hemodynamic (ie, phMRI) measures of brain function, these results corroborate the functional significance of the MRI study, and rule out potential spurious contributions arising from a putative direct vaso-active action of MOD.

Discrepancies between the imaging and cellular data are also to be noted, and differences in the neurophysiological processes underlying the two experimental readouts may be invoked to explain the lack of increased Fos induction in some areas found to be activated in the phMRI study (ie, raphe nuclei, somatosensory cortex and midline thalamus). Indeed, it has been shown that Fos induction does not always correspond to the activation shown by imaging techniques such as 2-deoxyglucose uptake mapping, or PET or blood oxygenation level-dependent contrast of MRI (Stark *et al.*, 2006; Cirelli and Tononi, 2000). Hemodynamic responses are generally thought to reflect local synaptic input (Logothetis *et al.*, 2001), whereas the *c-fos* gene and Fos protein induction is thought to reflect synaptic plasticity rather than neuronal firing *per se*, and does not occur in all CNS cell groups (Cirelli and Tononi, 2000).

Importantly, our Fos data provide additional evidence of an MOD-induced recruitment of fronto-cortical and striatal areas in the rodent brain. Similar findings have been observed with MOD (Scammell *et al.*, 2000; Willie *et al.*, 2005) or its metabolically active enantiomer armodafinil (Ficocchi *et al.*, 2009) in unanesthetized and unrestrained rodents, although this effect has not been consistently reported (Engber *et al.*, 1998; Lin *et al.*, 2000). At variance with previous reports (Scammell *et al.*, 2000; Engber *et al.*, 1998; Lin *et al.*, 2000), significant MOD-elicited Fos induction was not here observed in anterior and perifornical hypothalamic areas. On the other hand, significant Fos

induction was here documented in medial thalamic domains, which have not been previously reported to be recruited by MOD. Multiple procedural differences, and especially the use of anesthesia, may account for some of these discrepancies. It should however be emphasized that, as mentioned above, the neurochemical and regional effects of MOD are dose dependent (Ficocchi *et al.*, 2009; Scammell *et al.*, 2000). Therefore, the wide and heterogeneous spectrum of dose and routes of MOD administration employed in previous studies (5–600 mg/kg) could also have a role in the regional differences in the pattern of Fos activation.

In terms of a comparison with studies in unanesthetized animals, it has to be emphasized that previous studies have shown a negligible interference of halothane anesthesia with *c-fos* expression. For instance, halothane (1.5%), but not pentobarbital anesthesia preserved *c-fos* expression under resting conditions up to 2 h from induction (Marota *et al.*, 1992). Similarly, as also mentioned previously, halothane (1.5%) was found to preserve the spinal and supraspinal patterns of *c-fos* induced by mechanical stimulations (Novikova *et al.*, 2004). Halothane anesthesia also did not alter Fos expression in orexin-containing neurons compared with spontaneously breathing animals over 2 h exposure (Gompf *et al.*, 2009). Although these results do not permit to rule out an effect of anesthesia on Fos induction in our study, they however argue against a role of anesthesia as a main confounding factor in the interpretation of results. Additional Fos experiments using the same MOD formulation in unanesthetized and unrestrained animals are warranted to corroborate the significance of the results obtained at the cellular level in the present investigation in relation to previous studies in conscious rats.

Methodological Considerations and Limitations of the Study

The fact that our experiments were performed in anesthetized animals raise the question as to whether the observed effects truly reflect the pro-arousing and pro-cognitive action of MOD in conscious states. As also mentioned above concerning Fos induction, an experiment in freely moving animals would undoubtedly provide an important support to the present findings, overcoming the limitations related to the use of anesthesia. Such an experiment could, for example, be performed with CBF investigation using radiolabeled iodoantipyrine (Grunwald *et al.*, 1991). However, the iodoantipyrine technique suffers from some limitations, including the fact that, as other psychopharmacological measurements in behaving animals, it does not permit to differentiate the neural targets of the drug from the brain regions that underlie its secondary behavioral responses (eg, the activation of locomotor and autonomic centers by psychostimulant drugs). This aspect is of crucial importance for a translational approach such as that of our study.

On the other hand, multiple lines of evidence argue that the phMRI pattern here identified is representative of the central substrate recruited by MOD. First, the imaging and anesthetic protocol employed in our study has been repeatedly shown to preserve the features of the pattern of activity produced by a variety of psychoactive drugs with

remarkable correspondence between brain mapping in conscious animals and human fMRI results (reviewed by Bifone and Gozzi, 2010). For example, we were able to demonstrate that nicotine activates in the anesthetized rat the same cortico-limbic structures that express increased Fos induction in conscious animals (Mathieu-Kia et al, 1998) and are activated by the drug in humans as seen with fMRI (Stein et al, 1998; Gozzi et al, 2006). Similarly, in a recent series of phMRI studies with psychogenic antagonists of the N-methyl-D-aspartate receptor, such as ketamine and phencyclidine (Gozzi et al, 2008a, 2008b, 2008c), we have been able to highlight the activation of a cortico-limbic-thalamic network corresponding to the patterns of brain activity measured in freely moving rats with deoxyglucose mapping (Duncan et al, 1999) and in humans with different neuroimaging techniques (Deakin et al, 2008; Gozzi et al, 2008b; Langsjo et al, 2003).

Moreover, in the present study EEG recordings have shown that MOD could elicit a clear and robust pro-arousing signature despite the presence of the anesthetic. The observed increase in theta band power has been reliably described to reflect the activation of wakefulness-controlling brain areas in anesthetized animals (Shea et al, 2008; Morrison et al, 2011). Comparable increases in the theta band relative power and decreases in delta band power have been described with amphetamines in halothane-anesthetized animals (Berridge and Morris, 2000). This EEG signature is also observed following the presentation of arousing stimuli and seems to be dependent on the activation of the ascending noradrenergic pathways (Berridge and Foote, 1991). As changes in behavioral indices of arousal are accompanied by alterations in forebrain neuronal activity that are reflected in EEG signals (reviewed by Berridge, 2006), the observation of a wakefulness EEG signature demonstrates the efficacy of the MOD formulation used in the present experiments and provides a crucial intrinsic corroboration of the functional significance of the imaging findings.

Importantly, our imaging results also showed an encouraging spatial correspondence with analogous neuroimaging studies of MOD in humans. Specifically, in a recent randomized double-blind single photon emission computer tomography (SPECT) study, bilateral CBF increases have been shown in fronto-cortical areas, thalamic domains as well as dorsal raphe upon administration of MOD to healthy volunteers (Joo et al, 2008). Notably, all these regions have been shown to be activated by MOD in our study. Together, these lines of evidence converge to indicate that the pattern of activation identified here represents a plausible substrate for the wake-promoting and pro-cognitive effects of the drug.

CONCLUDING REMARKS

In conclusion, we used fMRI in the anesthetized rat to spatially resolve the neural circuitry activated by a dose of MOD that produces clinically relevant blood exposure. Our results show that MOD can focally and robustly activate fronto-cortical areas involved in higher cognitive functions, as well as a coordinated network of pro-arousing areas comprising dopamine-innervated cell groups. The functional significance of the imaging results was corroborated

by the presence of EEG desynchronization and enhanced Fos immunoreactivity in most of the brain regions identified in the imaging study. Collectively, these results provide a comprehensive description of the neural substrates for the established wake-promoting and pro-cognitive effects of the drug.

ACKNOWLEDGEMENTS

We would like to thank Valerio Crestan for his excellent technical support to the MRI study.

DISCLOSURE

Dino Montanari is an employee of GlaxoSmithKline. The authors declare that, except for income received from their primary employer, no financial support or compensation has been received from any individual or corporate entity over the past 3 years for research or professional service and there are no personal financial holdings that could be perceived as constituting a potential conflict of interest.

REFERENCES

- Antunes LM, Golledge HD, Roughan JV, Flecknell PA (2003). Comparison of electroencephalogram activity and auditory evoked responses during isoflurane and halothane anaesthesia in the rat. *Vet Anaesth Analg* 30: 15–23.
- Baranski JV, Pigeau R, Dinich P, Jacobs I (2004). Effects of modafinil on cognitive and meta-cognitive performance. *Hum Psychopharmacol* 19: 323–332.
- Becker JT, Olton DS, Anderson CA, Breiter ERP (1981). Cognitive mapping in rats: the role of the hippocampal and frontal systems in retention and reversal. *Behav Brain Res* 3: 1–22.
- Beracochea D, Cagnard B, Celerier A, le MJ, Peres M, Pierard C (2001). First evidence of a delay-dependent working memory-enhancing effect of modafinil in mice. *NeuroReport* 12: 375–378.
- Beracochea D, Celerier A, Peres M, Pierard C (2003). Enhancement of learning processes following an acute modafinil injection in mice. *Pharmacol Biochem Behav* 76: 473–479.
- Berridge CW (2006). Neural substrates of psychostimulant-induced arousal. *Neuropsychopharmacology* 31: 2332–2340.
- Berridge CW, Foote SL (1991). Effects of locus coeruleus activation on electroencephalographic activity in neocortex and hippocampus. *J Neurosci* 11: 3135–3145.
- Berridge CW, Morris MF (2000). Amphetamine-induced activation of forebrain EEG is prevented by noradrenergic beta-receptor blockade in the halothane-anesthetized rat. *Psychopharmacology* 148: 307–313.
- Bifone A, Gozzi A (2010). Functional and pharmacological MRI in understanding brain function. In: Hagan J (ed) *Molecular and Functional Models in Neuropsychiatry*. Springer, Berlin. pp 323–357.
- Bifone A, Gozzi A, Schwarz AJ (2010). Functional connectivity in the rat brain: a complex network approach. *Magn Reson Imaging* 28: 1200–1209.
- Birbaumer N, Murguialday AR, Cohen L (2008). Brain-computer interface in paralysis. *Curr Opin Neurol* 21: 634–638.
- Block AE, Dhanji H, Thompson-Tardif SF, Floresco SB (2007). Thalamic-prefrontal cortical-ventral striatal circuitry mediates dissociable components of strategy set shifting. *Cereb Cortex* 17: 1625–1636.

- Boxerman JL, Hamberg LM, Rosen BR, Weisskoff RM (1995). MR contrast due to intravascular magnetic susceptibility perturbations. *Magn Reson Med* 34: 555–566.
- Cirelli C, Tononi G (2000). On the functional significance of c-fos induction during the sleep-waking cycle. *Sleep* 23: 453–469.
- Dalley JW, Cardinal RN, Robbins TW (2004). Prefrontal executive and cognitive functions in rodents: neural and neurochemical substrates. *Neurosci Biobehav Rev* 28: 771–784.
- Dawson N, Thompson RJ, McVie A, Thomson DM, Morris BJ, Pratt JA (2010). Modafinil reverses phencyclidine-induced deficits in cognitive flexibility, cerebral metabolism, and functional brain connectivity. *Schizophr Bull*: doi:10.1093/schbul/sbq090.
- Deakin JFW, Lees J, McKie S, Hallak JEC, Williams SR, Dursun SM (2008). Glutamate and the neural basis of the subjective effects of ketamine: a pharmacological-magnetic resonance imaging study. *Arch Gen Psychiatry* 65: 154–164.
- de Saint HZ, Orosco M, Rouch C, Blanc G, Nicolaidis S (2001). Variations in extracellular monoamines in the prefrontal cortex and medial hypothalamus after modafinil administration: a microdialysis study in rats. *NeuroReport* 12: 3533–3537.
- Duncan GE, Miyamoto S, Leipziger JN, Lieberman JA (1999). Comparison of brain metabolic activity patterns induced by ketamine, MK-801 and amphetamine in rats: support for NMDA receptor involvement in responses to subanesthetic dose of ketamine. *Brain Res* 843: 171–183.
- Engber TM, Dennis SA, Jones BE, Miller MS, Contreras PC (1998). Brain regional substrates for the actions of the novel wake-promoting agent modafinil in the rat: comparison with amphetamine. *Neuroscience* 87: 905–911.
- Espana RA, Scammell TE (2004). Sleep neurobiology for the clinician. *Sleep* 27: 811–820.
- Ferrari L, Crestan V, Sabatini G, Vinco F, Fontana S, Gozzi A (2010). Brain penetration of local anaesthetics in the rat: Implications for experimental neuroscience. *J Neurosci Methods* 186: 143–149.
- Ferraro L, Fuxe K, Tanganelli S, Tomasini MC, Rambert FA, Antonelli T (2002). Differential enhancement of dialysate serotonin levels in distinct brain regions of the awake rat by modafinil: possible relevance for wakefulness and depression. *J Neurosci Res* 68: 107–112.
- Fiocchi EM, Lin YG, Aimone L, Gruner JA, Flood DG (2009). Armodafinil promotes wakefulness and activates Fos in rat brain. *Pharm Biochem Behav* 92: 549–557.
- Floresco SB, Ghods-Sharifi S, Vexelman C, Magyar O (2006). Dissociable roles for the nucleus accumbens core and shell in regulating set shifting. *J Neurosci* 26: 2449–2457.
- Fox MT, Barense MD, Baxter MG (2003). Perceptual attentional set-shifting is impaired in rats with neurotoxic lesions of posterior parietal cortex. *J Neurosci* 23: 676–681.
- Freudenreich O, Henderson DC, Macklin EA, Evins AE, Fan X, Cather C et al. (2009). Modafinil for clozapine-treated schizophrenia patients: a double-blind, placebo-controlled pilot trial. *J Clin Psychiatry* 70: 1674–1680.
- Friston KJ, Jezzard P, Turner R (1994). Analysis of functional MRI time-series. *Hum Brain Mapp* 1: 153–171.
- Gaisler-Salomon I, Schobel SA, Small SA, Rayport S (2009). How high-resolution basal-state functional imaging can guide the development of new pharmacotherapies for schizophrenia. *Schizophr Bull* 35: 1037–1044.
- Gold LH, Balster RL (1996). Evaluation of the cocaine-like discriminative stimulus effects and reinforcing effects of modafinil. *Psychopharmacology* 126: 286–292.
- Gompf H, Chen J, Sun Y, Yanagisawa M, Aston-Jones G, Kelz MB (2009). Halothane-induced hypnosis is not accompanied by inactivation of orexinergic output in rodents. *Anesthesiology* 111: 1001–1009.
- Gozzi A, Ceolin L, Schwarz A, Reese T, Bertani S, Bifone A (2007). A multimodality investigation of cerebral haemodynamics and autoregulation in pHMRI. *Magn Reson Imaging* 25: 826–833.
- Gozzi A, Crestan V, Turrini G, Clemens M, Bifone A (2010). Antagonism at serotonin 5-HT_{2A} receptors modulates functional activity of frontohippocampal circuit. *Psychopharmacology* 209: 37–50.
- Gozzi A, Herdon H, Schwarz A, Bertani S, Crestan V, Turrini G et al. (2008a). Pharmacological stimulation of NMDA receptors via co-agonist site suppresses fMRI response to phencyclidine in the rat. *Psychopharmacology* 201: 273–284.
- Gozzi A, Large C, Schwarz A, Bertani S, Crestan V, Bifone A (2008b). Differential effects of antipsychotic and glutamatergic agents on the pHMRI response to phencyclidine. *Neuropsychopharmacology* 33: 1690–1703.
- Gozzi A, Massagrande M, Amantini D, Antolini M, Martinelli P, Cesari N et al. (2011). Functional magnetic resonance imaging reveals different neural substrates for the effects of orexin-1 and orexin-2 receptor antagonists. *PLoS One* 6: 1e16406.
- Gozzi A, Schwarz A, Reese T, Bertani S, Crestan V, Bifone A (2006). Region-specific effects of nicotine on brain activity: a pharmacological MRI study in the drug-naïve rat. *Neuropsychopharmacology* 31: 1690–1703.
- Gozzi A, Schwarz AJ, Reese T, Crestan V, Bifone A (2008c). Drug-anaesthetic interaction in pHMRI: the case of the psychotomimetic agent phencyclidine. *Magn Reson Imaging* 26: 999–1006.
- Grassi-Zucconi G, Giuditta A, Mandile P, Chen S, Vescia S, Bentivoglio M (1994). c-fos spontaneous expression during wakefulness is reversed during sleep in neuronal subsets of the rat cortex. *J Physiol Paris* 88: 91–93.
- Grunwald F, Schrock H, Kuschinsky W (1991). The influence of nicotine on local cerebral blood flow in rats. *Neurosci Lett* 124: 108–110.
- Honey G, Bullmore E (2004). Human pharmacological MRI. *Trends Pharm Sci* 25: 366–374.
- Hudetz AG (2002). Effect of volatile anesthetics on interhemispheric EEG cross-approximate entropy in the rat. *Brain Res* 954: 123–131.
- Hunter MD, Ganesan V, Wilkinson ID, Spence SA (2006). Impact of modafinil on prefrontal executive function in schizophrenia. *Am J Psychiatry* 163: 2184–2186.
- Jasinski DR (2000). An evaluation of the abuse potential of modafinil using methylphenidate as a reference. *J Psychopharmacol* 14: 53–60.
- Joo EY, Tae WS, Jung KY, Hong SB (2008). Cerebral blood flow changes in man by wake-promoting drug, modafinil: a randomized double blind study. *J Sleep Res* 17: 82–88.
- Kruszewski SP (2006). Euphorogenic and abusive properties of modafinil. *Am J Psychiatry* 163: 549.
- Kumar R (2008). Approved and investigational uses of modafinil: an evidence-based review. *Drugs* 68: 1803–1839.
- Langsjo JW, Kaisti KK, Aalto S, Hinkka S, Aantaa R, Oikonen V et al. (2003). Effects of subanesthetic doses of ketamine on regional cerebral blood flow, oxygen consumption, and blood volume in humans. *Anesthesiology* 99: 614–623.
- Lin JS, Gervasoni D, Hou Y, Vanni-Mercier G, Rambert F, Frydman A (2000). Effects of amphetamine and modafinil on the sleep/wake cycle during experimental hypersomnia induced by sleep deprivation in the cat. *J Sleep Res* 9: 89–96.
- Lin JS, Hou Y, Jouvet M (1996). Potential brain neuronal targets for amphetamine-, methylphenidate-, and modafinil-induced wakefulness, evidenced by c-fos immunocytochemistry in the cat. *Proc Natl Acad Sci USA* 93: 14128–14133.
- Logothetis NK, Pauls J, Augath M, Trinath T, Oeltermann A (2001). Neurophysiological investigation of the basis of the fMRI signal. *Nature* 412: 150–157.
- Lynch G, Palmer LC, Gall CM (2011). The likelihood of cognitive enhancement. *Pharmacol Biochem Behav* 99: 116–129.
- Madras BK, Xie Z, Lin Z, Jassen A, Panas H, Lynch L et al. (2006). Modafinil occupies dopamine and norepinephrine transporters

- in vivo* and modulates the transporters and trace amine activity *in vitro*. *J Pharmacol Exp Ther* 319: 561–569.
- Mandeville JB, Marota JJA, Kosofsky BE, Keltner JR, Weissleder R, Rosen B et al. (1998). Dynamic functional imaging of relative cerebral blood volume during rat forepaw stimulation. *Magn Reson Med* 39: 615–624.
- Marota JJ, Crosby G, Uhl GR (1992). Selective effects of pentobarbital and halothane on c-fos and jun-B gene expression in rat brain. *Anesthesiology* 77: 365–371.
- Mathieu-Kia AM, Pages C, Besson MJ (1998). Inducibility of c-Fos protein in visuo-motor system and limbic structures after acute and repeated administration of nicotine in the rat. *Synapse* 29: 343–354.
- McClellan KJ, Spencer CM (1998). Modafinil: a review of its pharmacology and clinical efficacy in the management of narcolepsy. *CNS Drugs* 9: 311–324.
- McCormick DA, Bal T (1997). Sleep and arousal: thalamocortical mechanisms. *Annu Rev Neurosci* 20: 185–215.
- Mesulam MM (1990). Large-scale neurocognitive networks and distributed processing for attention, language, and memory. *Ann Neurol* 28: 597–613.
- Minzenberg MJ, Carter CS (2007). Modafinil: a review of neurochemical actions and effects on cognition. *Neuropsychopharmacology* 33: 1477–1502.
- Morrison PD, Nottage J, Stone JM, Bhattacharyya S, Tunstall N, Brenneisen R et al. (2011). Disruption of frontal theta coherence by [delta]9-tetrahydrocannabinol is associated with positive psychotic symptoms. *Neuropsychopharmacology* 36: 827–836.
- Murillo-Rodriguez E, Haro R, Palomero-Rivero M, Millan-Aldaco D, Drucker-Colin R (2007). Modafinil enhances extracellular levels of dopamine in the nucleus accumbens and increases wakefulness in rats. *Behav Brain Res* 176: 353–357.
- Myrick H, Malcolm R, Taylor B, LaRowe S (2004). Modafinil: preclinical, clinical, and post-marketing surveillance—a review of abuse liability issues. *Ann Clin Psychiatry* 16: 101–109.
- Newman JL, Negus SS, Lozama A, Prisinzano TE, Mello NK (2010). Behavioral evaluation of modafinil and the abuse-related effects of cocaine in rhesus monkeys. *Exp Clin Psychopharmacol* 18: 395–408.
- Novikova NS, Kazakova TB, Rogers V, Korneva EA (2004). Expression of the c-fos gene in spinal cord and brain cells in rats subjected to stress in conditions of exposure to various types of halothane anesthesia. *Neurosci Behav Phys* 34: 407–412.
- Pace-Schott EF, Hobson JA (2002). The neurobiology of sleep: genetics, cellular physiology and subcortical networks. *Nat Rev Neurosci* 3: 591–605.
- Paxinos G, Watson C (2005). *The Rat Brain in Stereotaxic Coordinates*, 5th edn, Elsevier, Berlin.
- Pepelko WE, Dixon GA (1975). Arterial blood gases in conscious rats exposed to hypoxia, hypercapnia, or both. *J Appl Physiol* 38: 581–587.
- Pierre JM, Peloian JH, Wirshing DA, Wirshing WC, Marder SR (2007). A randomized, double-blind, placebo-controlled trial of modafinil for negative symptoms in schizophrenia. *J Clin Psychiatry* 68: 705–710.
- Pigeau R, Naitoh P, Buguet A, McCann C, Baranski J, Taylor M (1995). Modafinil, d-amphetamine and placebo during sustained mental work: Effects on mood, fatigue, cognitive performance and body temperature. *J Sleep Res* 4: 212–228.
- Qu WM, Huang ZL, Xu XH, Matsumoto N, Urade Y (2008). Dopaminergic D1 and D2 receptors are essential for the arousal effect of modafinil. *J Neurosci* 28: 8462–8469.
- Ramos-Cabrer P, Weber R, Wiedermann D, Hoehn M (2005). Continuous noninvasive monitoring of transcutaneous blood gases for a stable and persistent BOLD contrast in fMRI studies in the rat. *NMR Biomed* 18: 440–446.
- Repantis D, Schlattmann P, Laisney O, Heuser I (2010). Modafinil and methylphenidate for neuroenhancement in healthy individuals: a systematic review. *Pharmacol Res* 62: 187–206.
- Salamone JD, Correa M (2002). Motivational views of reinforcement: implications for understanding the behavioral functions of nucleus accumbens dopamine. *Behav Brain Res* 137: 3–25.
- Saletu M, Anderer P, Saletu-Zyhlarz GM, Mandl M, Arnold O, Zeitlhofer J (2004). EEG-tomographic studies with LORETA on vigilance differences between narcolepsy patients and controls and subsequent double-blind, placebo-controlled studies with modafinil. *J Neurol* 251: 1354–1363.
- Saletu M, Anderer P, Semlitsch HV, Saletu-Zyhlarz GM, Mandl M, Zeitlhofer J (2007). Low-resolution brain electromagnetic tomography (LORETA) identifies brain regions linked to psychometric performance under modafinil in narcolepsy. *Psychiatry Res* 154: 69–84.
- Scammell TE, Estabrooke IV, McCarthy MT, Chemelli RM, Yanagisawa M, Miller MS (2000). Hypothalamic arousal regions are activated during modafinil-induced wakefulness. *J Neurosci* 20: 8620–8628.
- Schwarz AJ, Danckaert A, Reese T, Gozzi A, Paxinos G, Watson C et al. (2006a). A stereotaxic MRI template set for the rat brain with tissue class distribution maps and co-registered anatomical atlas: application to pharmacological MRI. *Neuroimage* 32: 538–550.
- Schwarz AJ, Gozzi A, Bifone A (2009). Community structure in networks of functional connectivity: resolving functional organization in the rat brain with pharmacological MRI. *Neuroimage* 47: 302–311.
- Schwarz AJ, Gozzi A, Reese T, Bifone A (2007a). Functional connectivity in the pharmacologically activated brain: resolving networks of correlated responses to d-amphetamine. *Magn Reson Med* 57: 704–713.
- Schwarz AJ, Gozzi A, Reese T, Bifone A (2007b). *In vivo* mapping of functional connectivity in neurotransmitter systems using pharmacological MRI. *Neuroimage* 34: 1627–1636.
- Schwarz AJ, Reese T, Gozzi A, Bifone A (2003). Functional MRI using intravascular contrast agents: detrending of the relative cerebrovascular (rCBV) time course. *Magn Reson Imaging* 21: 1191–1200.
- Schwarz AJ, Whitcher B, Gozzi A, Reese T, Bifone A (2006b). Study-level wavelet cluster analysis and data-driven signal models in pharmacological MRI. *J Neurosci Methods* 159: 346–360.
- Shea JL, Mochizuki T, Sagvaag V, Aspevik T, Bjorkum AA, Datta S (2008). Rapid eye movement (REM) sleep homeostatic regulatory processes in the rat: changes in the sleep-wake stages and electroencephalographic power spectra. *Brain Res* 1213: 48–56.
- Small SA, Chawla MK, Buonocore M, Rapp PR, Barnes CA (2004). Imaging correlates of brain function in monkeys and rats isolates a hippocampal subregion differentially vulnerable to aging. *Proc Natl Acad Sci USA* 101: 7181–7186.
- Smith SM, Jenkinson M, Woolrich MW, Beckmann CF, Behrens TE, Johansen-Berg H et al. (2004). Advances in functional and structural MR image analysis and implementation as FSL. *Neuroimage* 23(Suppl 1): S208–S219.
- Spence SA, Green RD, Wilkinson ID, Hunter MD (2005). Modafinil modulates anterior cingulate function in chronic schizophrenia. *Br J Psychiatry* 187: 55–61.
- Squire LR (1992). Memory and the hippocampus: a synthesis from findings with rats, monkeys, and humans. *Psychol Rev* 99: 195–231.
- Stark JA, Davies KE, Williams SR, Luckman SM (2006). Functional magnetic resonance imaging and c-Fos mapping in rats following an anorectic dose of m-chlorophenylpiperazine. *Neuroimage* 31: 1228–1237.
- Stein EA, Pankiewicz J, Harsch HH, Cho JK, Fuller SA, Hoffmann RG et al. (1998). Nicotine-induced limbic cortical activation in the human brain: a functional MRI study. *Am J Psychiatry* 155: 1009–1015.
- Steriade M (1996). Arousal: revisiting the reticular activating system. *Science* 272: 225–226.

- Steriade M, Amzica F, Contreras D (1994). Cortical and thalamic cellular correlates of electroencephalographic burst-suppression. *Electroenceph Clin Neurophysiol* **90**: 1–16.
- Stoops W, Lile J, Fillmore M, Glaser P, Rush C (2005). Reinforcing effects of modafinil: influence of dose and behavioral demands following drug administration. *Psychopharmacology* **182**: 186–193.
- Sumner BEH, Cruise LA, Slattery DA, Hill DR, Shahid M, Henry B (2004). Testing the validity of c-fos expression profiling to aid the therapeutic classification of psychoactive drugs. *Psychopharmacology* **171**: 306–321.
- Sun WZ, Shyu BC, Shieh JY (1996). Nitrous oxide or halothane, or both, fail to suppress c-fos expression in rat spinal cord dorsal horn neurones after subcutaneous formalin. *Br J Anaesth* **76**: 99–105.
- Thomas RJ, Kwong K (2006). Modafinil activates cortical and subcortical sites in the sleep-deprived state. *Sleep* **29**: 1471–1481.
- Tsanov M, Lyons DG, Barlow S, Gonz lez Reyes RE, O'Mara SM (2007). The psychostimulant modafinil facilitates water maze performance and augments synaptic potentiation in dentate gyrus. *Neuropharmacology* **59**: 9–19.
- Turner DC, Robbins TW, Clark L, Aron AR, Dowson J, Sahakian BJ (2003). Cognitive enhancing effects of modafinil in healthy volunteers. *Psychopharmacology* **165**: 260–269.
- Uylings HB, Groenewegen HJ, Kolb B (2003). Do rats have a prefrontal cortex? *Behav Brain Res* **146**: 3–17.
- Vanderwolf CH (1992). The electrocorticogram in relation to physiology and behavior: A new analysis. *Electroenceph Clin Neurophysiol* **82**: 165–175.
- Vertes RP (2006). Interactions among the medial prefrontal cortex, hippocampus and midline thalamus in emotional and cognitive processing in the rat. *Neuroscience* **142**: 1–20.
- Volkow ND, Fowler JS, Logan J, Alexoff D, Zhu W, Telang F et al. (2009). Effects of modafinil on dopamine and dopamine transporters in the male human brain. *JAMA* **301**: 1148–1154.
- Weiergrasber M, Henry M, Hescheler J, Smyth N, Schneider T (2005). Electrocorticographic and deep intracerebral EEG recording in mice using a telemetry system. *Brain Res Protoc* **14**: 154–164.
- Wesensten NJ, Belenky G, Kautz MA, Thorne DR, Reichardt RM, Balkin TJ (2002). Maintaining alertness and performance during sleep deprivation: modafinil vs caffeine. *Psychopharmacology* **159**: 238–247.
- Willie JT, Renthal W, Chemelli RM, Miller MS, Scammell TE, Yanagisawa M (2005). Modafinil more effectively induces wakefulness in orexin-null mice than in wild-type littermates. *Neuroscience* **130**: 983–995.
- Wisor JP, Nishino S, Sora I, Uhl GH, Mignot E, Edgar DM (2001). Dopaminergic role in stimulant-induced wakefulness. *J Neurosci* **21**: 1787–1794.
- Wong YN, Simcoe D, Hartman LN, Laughton WB, King SP, McCormick GC (1999). A double-blind, placebo-controlled, ascending-dose evaluation of the pharmacokinetics and tolerability of modafinil tablets in healthy male volunteers. *J Clin Pharmacol* **39**: 30–40.
- Worsley KJ, Evans AC, Marrett S, Neelin P (1992). A three-dimensional statistical analysis for CBF activation studies in human brain. *J Cereb Blood Flow Metab* **12**: 900–918.
- Yu E, Chovan JP, Ring SC, Robertson P (2000). Pharmacokinetics of modafinil enantiomers in rats. *AAPS J* **2**: 3337–3340.
- Zaharchuk G, Mandeville JB, Bogdanov Jr AA, Weissleder R, Rosen BR, Marota JJ (1999). Cerebrovascular dynamics of autoregulation and hypoperfusion. An MRI study of CBF and changes in total and microvascular cerebral blood volume during hemorrhagic hypotension. *Stroke* **30**: 2197–2204.

Supplementary Information accompanies the paper on the Neuropsychopharmacology website (<http://www.nature.com/npp>)